To appear in *Molecular Physics*
Vol. 00, No. 00, Month 2013, 1–19

RESEARCH ARTICLE

The falling cat problem and shape effects in small molecules in a random environment: a case study

Carsten Hartmann*,[a] , Tomohiro Yanao[b]

[a] *Institute of Mathematics, Freie Universität Berlin, 14195 Berlin, Germany*
[b] *Dpt. of Applied Mechanics and Aerospace Engineering, Waseda University, Tokyo, Japan*
(*Received 00 Month 200x; final version received 00 Month 200x*)

We study the coupling between shape changes and rotations of molecules in a random environment. As a prototype of molecules or biopolymers that can undergo nontrivial conformational transitions we consider a planar four-atomic molecule, with underdamped dynamics of Langevin-type. In this simplified setting, we can extend the available gauge theory of semi-flexible molecules to the stochastic setting which allows us to analyze and explain geometric phase effects that arise from the internal motion of the molecule. Due to the stochastic nature of the Langevin system, the internal dynamics contains temperature-dependent coriolis forces that arise from the fluctuations of the angular momentum around its mean value zero. All theoretical investigations are supplemented by numerical simulations, in which we specifically investigate the dependence of the orientational shift on the parameters of the Langevin equation, i.e. friction coefficient, atomic masses, temperature, and the velocity of deformation of the system. The numerical results confirm our theoretical findings. We further discuss various extension of the analysis, e.g. to the overdamped limit or optimal control.

1. Introduction

Conformational transitions of molecules are essential in chemical reactions, self-organization of nanomaterials and mechanical functions of biomolecules. Even though significant advancements have been made in both theoretical and computational methods for molecular dynamics, a quite fundamental issue intrinsic to the dynamics of flexible bodies seems to be highly unexplored, that is, the geometric phase effect. As is known, a cat can change its orientation in space while it is falling. This effect, known as the *falling cat* effect, is interesting because the cat achieves the flip-flop under the conditions of zero total angular momentum [10]. The falling cat effect is a typical instance of the fact that changes in the shape of a flexible body can give rise to changes in its orientation [15]. Geometric phase effects of this kind are known in engineering and utilized in the attitude control of mechanical systems, such as space robots and satellites [11]; similar geometric phases are known to play a crucial role in the propulsion of micro-organisms or fishs in fluids [17]. In terms of the conformational dynamics of molecules, however, little attention has been paid to the role of such geometric phase effects; cf. [21, 22]. In point of fact many methodologies of molecular dynamics try to disregard geometric phases by invoking explicit approximations or conventions, such as the Eckart conditions [4, 18], that exclude coupling between internal vibrations of molecules and and their orientation.

The purpose of this study therefore is to understand and quantify geometric

*Corresponding author. Email: chartman@mi.fu-berlin.de

ISSN: 00268976 print/ISSN 13623028 online

DOI: 10.1080/0026897YYxxxxxxxx
http://www.informaworld.com

phase effects in the stochastic dynamics of molecules. Specifically, we plan to address the following questions: (1) How can we separate the shape dynamics and rotations of molecules in solvents? (2) Can we employ symmetry reduction tools as in geometric mechanics to obtain reduced shape dynamics? (3) Do the geometric objects on shape space known in geometric mechanics, such as curvature and gauge potentials, play a role in the Langevin dynamics of molecules? (4) What is the relationship between the Fixman potential and the geometry of shape space?

2. Gauge theory of semiflexible molecules in a random environment

Before we discuss stochastic dynamical properties of molecular systems, we briefly analyze the kinematics of flexible or semi flexible (i.e. with fixed bond lengths) molecules. Molecules can be modelled as systems of, say, n point-like particles that interact via smooth or non-smooth potentials. If no external forces are present all forces involved are equivariant under overall translations and rotations of the molecule. As a consequence, of the $3n$ degrees of freedom that the molecule possesses, three can be eliminated on the basis of translational invariance and two more on the basis of rotational invariance [13]. Note that, although the rotation group is three-dimensional, the fact that rotations around the three principal axes do not commute in general allows only for the elimination of two rotational degrees of freedom. A notable exception is when the molecule has zero total angular momentum, in which case all three rotational degrees of freedom can be removed; see [14] and the references therein.

One might be tempted to think that, because of the symmetry, rotations do not play a role for the conformational dynamics of a molecule that involves only internal degrees of freedom. This view is supported by the fact that the typical visualization tool for molecular dynamics trajectories remove overall translations and rotations by aligning the molecules with respect to their initial reference configuration, using rigid body transformations (i.e., translations and rotations) or that some molecular dynamics algorithms use explicit coordinate conventions by which the coupling between internal variables and rotations and translations is removed (cf. [20]). Nevertheless it is well-known that internal and external coordinates are coupled, in that shape changes of a multibody system can give rise to a change of orientation [13]. The most prominent example is the example of a falling cat that can turn itself right-side-up as it falls, no matter which way up it was initially and without having angular momentum.

Geometric phase and gauge potential Another example of shape-orientation coupling is the semi-flexible planar molecule depicted in Figure 1, which configurations are completely specified by the two bond angles α and β, the orientation of the central bond with respect to one of the coordinate axes and the centre of mass; the shape space of the molecule is the two-dimensional torus $\mathbf{T}^2 = S^1 \times S^1$. Figure 2 below shows a cyclic shape transformation of the molecule under zero angular momentum that results in a change of orientation. The corresponding orbit in the two-dimensional shape space is shown in Figure 3.

Let us analyze the example in detail. For simplicity we assume that the bond lengths $b > 0$ between two neighbouring atoms are all equal and that all atoms have the same mass $m > 0$. Without loss of generality we assume that the centre of mass is at the origin of the space fixed coordinate system. To specify the orientation of the molecule we introduce a body-fixed frame by an orthogonal 2×2 matrix $Q = (\boldsymbol{e}_x, \boldsymbol{e}_y)$ where the x-axis of the frame, $\boldsymbol{e}_x$, is parallel to the vector connecting

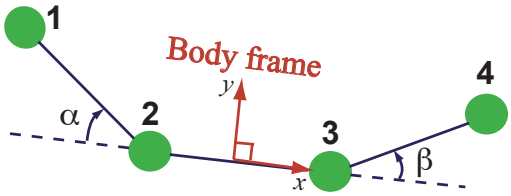

Figure 1. Semiflexible four-atomic molecule in the plane and the coordinate and body-frame conventions

particle 2 and 3, whereas the y-axis, $\boldsymbol{e}_y$, is orthogonal to $\boldsymbol{e}_x$ and centred between atoms number 2 and 3. The positions of the four atoms with respect to the body frame are then given by

$$\begin{aligned} \boldsymbol{r}_1 &= (-b/2 - b\cos\alpha, b\sin\alpha)^T \\ \boldsymbol{r}_2 &= (-b/2, 0)^T \\ \boldsymbol{r}_3 &= (b/2, 0)^T \\ \boldsymbol{r}_4 &= (b/2 + b\cos\beta, b\sin\beta)^T . \end{aligned} \tag{2.1}$$

The angular momentum with respect to the body frame is given by

$$L = \Theta\left(\omega + A_1\dot{\alpha} + A_2\dot{\beta}\right) \tag{2.2}$$

where Θ is the moment of inertia, $\omega = \dot{\theta}$ is the angular velocity of the body frame, with θ being the angle between the body-fixed and reference coordinate axes and

$$Q = \begin{pmatrix} \cos\theta & -\sin\theta \\ \sin\theta & \cos\theta \end{pmatrix}$$

(Note that $\omega = \boldsymbol{e}_y \cdot \dot{\boldsymbol{e}}_x = -\dot{\boldsymbol{e}}_y \cdot \boldsymbol{e}_x$.) With some little algebra, the coefficients A_1 and A_2 of the *gauge potential* that will be defined later on, can be explicitly computed:

$$\begin{aligned} A_1 &= \frac{3 + 2\cos\alpha + \cos(\alpha+\beta)}{10 + 4\cos\alpha + 4\cos\beta + 2\cos(\alpha+\beta)} \\ A_2 &= \frac{3 + 2\cos\beta + \cos(\alpha+\beta)}{10 + 4\cos\alpha + 4\cos\beta + 2\cos(\alpha+\beta)} . \end{aligned}$$

The condition of zero angular momentum is equivalent to the vanishing of the term in the parenthesis in (2.2) which, using that $d\theta = \omega dt$ implies that

$$d\theta = -(A_1 d\alpha + A_2 d\beta) . \tag{2.3}$$

Now suppose that $c\colon [0,T] \to \mathbf{T}^2$, $c = (\alpha, \beta)$ is a curve on the torus, i.e. in shape space. If the curve is closed—which amounts to a cyclic shape change—we can compute the net change of the orientation of the tetramer by integrating (2.3) over the closed curve, say, $\gamma = \{c(t)\colon 0 \le t \le T,\, c(0) = c(T)\}$, i.e.,

$$\Delta\theta = -\oint_\gamma (A_1 d\alpha + A_2 d\beta)$$

For the cyclic shape change depicted in Figure 3, the net change in orientation under zero angular momentum is found to be $\Delta\theta = 11.786°$. A series of snapshots

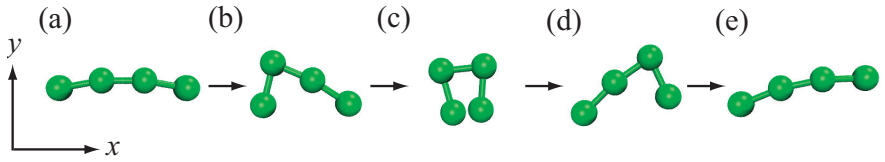

Figure 2. Cyclic shape change of four atoms confined to the plane at zero angular momentum.

of the molecule is shown in Figure 2; as can be seen, the molecule rotates while undergoing a shape transformation. That is, even though the curve may be closed in shape space, it does not closed in configuration space.

An important aspect of our little example is that the orientational shift is a purely geometric effect, called *Berry phase* or *Hannay-Berry phase* that is well-known in quantum mechanics [2, 16]. It is moreover intrinsic, in that it is independent of the choice of frame or reference configuration. Here we are interested in the case that the molecules are embedded in a solvent of, say, water molecules that can be described by random noise and dissipation acting on the molecule. The question then is whether the geometric phase persists under these conditions, especially if the noise is spatially isotropic, so that the angular momentum of the molecule is zero on average.

2.1. *Langevin dynamics of a semiflexible molecule*

We go back to a generic flexible molecule, consisting of n atoms moving in a d-dimensional configuration space where $d = 2$ in case of a planar molecule and $d = 3$ otherwise. The phase space then is $U \times \mathbf{R}^{nd}$, with $U \subset \mathbf{R}^{nd}$ denoting the nd-dimensional configuration space of the molecule. For simplicity we assume that all particles have the same mass $m > 0$. Now let

$$H\colon U \times \mathbf{R}^{nd} \to \mathbf{R}\,, \quad H(\boldsymbol{q},\boldsymbol{p}) = \frac{1}{2m}\sum_{i=1}^{n} |\boldsymbol{p}_i|^2 + V(\boldsymbol{q}) \tag{2.4}$$

denote the system Hamiltonian where $V\colon U \to \mathbf{R}$ is a smooth potential that is bounded from below and $\boldsymbol{p}_i \in \mathbf{R}^d$ is the momentum of the i-th particle, conjugate to $\boldsymbol{q}_i$. We suppose that the dynamics are governed by a Langevin equation of the form (using the usual physics notation for Itô stochastic differential equations)

$$\begin{aligned} \dot{\boldsymbol{q}}_i &= \frac{\partial H}{\partial \boldsymbol{p}_i} \\ \dot{\boldsymbol{p}}_i &= -\frac{\partial H}{\partial \boldsymbol{q}_i} - \gamma\frac{\partial H}{\partial \boldsymbol{p}_i} + \sigma\boldsymbol{\xi}_i(t)\,, \quad i = 1,\dots,n\,, \end{aligned} \tag{2.5}$$

where $\boldsymbol{\xi} = (\boldsymbol{\xi}_1,\dots,\boldsymbol{\xi}_n)$ is nd-dimensional Gaussian white noise and $\gamma, \sigma > 0$ are scalar friction and noise coefficients. Without loss of generality we assume that $\sigma > 0$ and that $2\vartheta\gamma = \sigma^2$ for some $\vartheta > 0$, which implies that the unique ergodic stationary distribution of the Langevin equation has the density

$$\rho(\boldsymbol{q},\boldsymbol{p}) = \frac{1}{Z}\exp(-\vartheta^{-1}H(\boldsymbol{q},\boldsymbol{p}))\,. \tag{2.6}$$

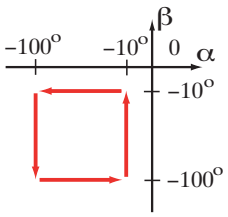

Figure 3. Shape transformation shown in Figure 2: closed curve on the 2-torus.

Here Z is a normalizing constant that normalizes the total probability to one:

$$\int_{U\times\mathbf{R}^{nd}} \rho(\boldsymbol{q},\boldsymbol{p})\, d\boldsymbol{q}d\boldsymbol{p} = 1$$

2.2. *Coordinate expressions: Shape and rigid body motion of the tetramer*

We now want to repeat the procedure discussed in the previous section for our four-atomic model molecule for the case of Langevin dynamics, i.e., we consider the case $d = 2$ and $n = 4$. The aim is to arrive at an explicit form of the Langevin equation of the tetramer in terms of shape coordinates and rotation and translation coordinates, from which one can read off the geometric phase that the molecule undergoes during shape transformations.[1]

It is helpful to bear in mind that the Langevin equation (2.5) is covariant under point transformations: Given a coordinate transformation $F\colon X \to Q$ with $\boldsymbol{q} = F(\boldsymbol{x})$ it follows that the Langevin equation in terms of the new configuration variables $\boldsymbol{x}$ and their conjugate momenta $\boldsymbol{y}$ is again of the form [7]

$$\begin{aligned} \dot{\boldsymbol{x}}_i &= \frac{\partial \tilde{H}}{\partial \boldsymbol{y}_i} \\ \dot{\boldsymbol{y}}_i &= -\frac{\partial \tilde{H}}{\partial \boldsymbol{x}_i} - \sum_{j=1}^{3} \tilde{\gamma}_{ij} \frac{\partial \tilde{H}}{\partial \boldsymbol{y}_j} + \sum_{j=1}^{3} \tilde{\sigma}_{ij} \boldsymbol{\xi}_j\,, \quad i = 1,\dots,n\,, \end{aligned} \tag{2.7}$$

where $\tilde{H}(\boldsymbol{x},\boldsymbol{y})$ is the Hamiltonian expressed in the new coordinates

$$\boldsymbol{x} = F^{-1}(\boldsymbol{q}) \quad \text{and} \quad \boldsymbol{y} = (\nabla F(F^{-1}(\boldsymbol{q}))^T \boldsymbol{p}$$

and $\tilde{\gamma} = \nabla F^T \gamma \nabla F$, $\tilde{\sigma} = \nabla F^T \sigma$ are the new friction and noise coefficients. It can be readily seen that the transformed coefficients satisfy

$$2\vartheta\tilde{\gamma} = \tilde{\sigma}\tilde{\sigma}\,. \tag{2.8}$$

Note, however, that $\tilde{\gamma}$ and $\tilde{\sigma}$ may depend on the new coordinates $\boldsymbol{x}$.

We now proceed in two steps. Firstly, we split off the translational degree of freedom, that turns out to be irrelevant for the subsequent analysis, in a second step we divide the phase space into rotational and shape coordinates; as one might expect the two latter are intrinsically coupled which gives rise to a geometric phase.

[1]The restriction to planar molecules is to keep the notation transparent and to avoid unnecessary technical details, such as non-canonical coordinates or anholonomic frames; see [13] for a discussion of the general case.

Step one: translations. To handle translations we introduce mass-weighted Jacobi coordinates that are popular in quantum mechanics [23] and celestial mechanics [1] and that turn out to be a convenient choice as they diagonalize the kinetic energy. The idea is to form pairwise clusters of atoms and to use their barycentres as new coordinates; this step is then iterated, building pairs between the barycentres and so on. Specifically, calling G the linear transformation that defines the Cartesian coordinates $\boldsymbol{q} = (\boldsymbol{q}_1, \dots, \boldsymbol{q}_4)$ in terms of the Jacobi vector $\boldsymbol{\rho} = (\boldsymbol{\rho}_1, \boldsymbol{\rho}_2, \boldsymbol{\rho}_3)$ plus the centre of mass $\boldsymbol{R}$, it follows that the Hamiltonian can be split according to [22]

$$\tilde{H}(\boldsymbol{\rho}, \boldsymbol{R}, \boldsymbol{\pi}, \boldsymbol{P}) = \frac{1}{2M}|\boldsymbol{P}|^2 + \frac{1}{2}|\boldsymbol{\pi}|^2 + \tilde{V}(\boldsymbol{\rho})\,,$$

where $\tilde{V}(\boldsymbol{\rho}) = V(G(\boldsymbol{\rho}, \boldsymbol{R}))$ is the potential expressed in the Jacobi coordinates and M is the total mass. In our the case the first three mass-weighted Jacobi vectors and the centre of mass read

$$\begin{aligned}
\boldsymbol{\rho}_1 &= \sqrt{\frac{m}{2}}(\boldsymbol{q}_2 - \boldsymbol{q}_1) \\
\boldsymbol{\rho}_2 &= \sqrt{\frac{m}{2}}(\boldsymbol{q}_4 - \boldsymbol{q}_3) \\
\boldsymbol{\rho}_3 &= \sqrt{m}\left(\frac{1}{2}(\boldsymbol{q}_1 + \boldsymbol{q}_2) - \frac{1}{2}(\boldsymbol{q}_3 + \boldsymbol{q}_4)\right) \\
\boldsymbol{R} &= \frac{\boldsymbol{q}_1 + \boldsymbol{q}_2 + \boldsymbol{q}_3 + \boldsymbol{q}_4}{4}\,,
\end{aligned}$$

and it can be readily checked that, with this choice of coordinates, the translational motion separates from the rest of the Hamiltonian, and thus can be ignored in the following. Transforming noise and friction coefficients is now straightforward: Letting $J \in \mathbf{R}^{4\times 3}$ denote the constant Jacobian of the linear map $\boldsymbol{\rho} \mapsto G(\boldsymbol{\rho}, \cdot)$, and noting that $J^T J = m^{-1}\mathrm{Id}_{3\times 3}$ we have

$$\tilde{\gamma} = \frac{\gamma}{m}\,, \quad \tilde{\sigma} = \frac{\sigma}{\sqrt{m}}$$

In terms of the Jacobi coordinates $\boldsymbol{\rho} = (\boldsymbol{\rho}_1, \boldsymbol{\rho}_2, \boldsymbol{\rho}_3)$ and their conjugate momenta $\boldsymbol{\pi} = (\boldsymbol{\pi}_1, \boldsymbol{\pi}_2, \boldsymbol{\pi}_3)$, the Langevin equation reads

$$\begin{aligned}
\dot{\boldsymbol{\rho}}_i &= \frac{\partial \tilde{H}}{\partial \boldsymbol{\pi}_i} \\
\dot{\boldsymbol{\pi}}_i &= -\frac{\partial \tilde{H}}{\partial \boldsymbol{\rho}_i} - \tilde{\gamma}\frac{\partial \tilde{H}}{\partial \boldsymbol{\pi}_i} + \tilde{\sigma}\boldsymbol{\xi}_i\,, \quad i = 1, \dots, 3\,,
\end{aligned} \tag{2.9}$$

where

$$\tilde{H}(\boldsymbol{\rho}, \boldsymbol{\pi}) = \frac{1}{2}|\boldsymbol{\pi}|^2 + \tilde{V}(\boldsymbol{\rho})$$

is the original Hamiltonian without the translational part.

Remark. In general the fact that the Hamiltonian can be separated does not imply that friction and noise coefficients are block diagonal or even diagonal, i.e., the

centre of mass motion can still be coupled to the other degrees of freedom via friction and noise. This is the case when not all atomic masses are equal, even though γ, σ in the Langevin equation (2.5) are scalar. That is, even though the transformation to Jacobi coordinates removes the masses from the kinetic energy of the Hamiltonian, it renders potential energy and the dissipative forces to be mass dependent. But as the coupling between the centre of mass and the three Jacobi vectors is linear, the mean value of the linear momentum P associated with the centre of mass is zero in equilibrium, and it is always safe to ignore its motion.[1]

Step two: shape coordinates and rotations. In general it requires $3n-6$ coordinates to specify the shape of a fully flexible n-atomic molecule. In our case we assume that the bonds are rigid and that the molecule is confined to the plane, leaving 5 degrees of freedom in total (2 shape coordinates, 2 for translation, 1 for rotation). Ignoring translations, we have only 3 degrees of freedom left, and we can fully specify the Jacobi vectors $\boldsymbol{\rho}_1, \ldots, \boldsymbol{\rho}_3$ by the two shape coordinates $s = (\alpha, \beta)$ and the orientation θ. We adopt the following convention and express any configuration of our molecule by

$$\boldsymbol{\rho}_i = Q(\theta)\tilde{\boldsymbol{\rho}}_i(s)\,, i = 1, 2, 3\,,$$

where Q is a 2×2 rotation matrix that specifies the relative orientation θ of the body frame, and $\tilde{\boldsymbol{\rho}}$ is the collection of Jacobi vectors in the body fixed frame, i.e.,

$$\begin{aligned}
\tilde{\boldsymbol{\rho}}_1 &= b\sqrt{\frac{m}{2}}\,(\cos\alpha,\, -\sin\alpha)^T \\
\tilde{\boldsymbol{\rho}}_2 &= b\sqrt{\frac{m}{2}}\,(\cos\beta,\, \sin\beta)^T \\
\tilde{\boldsymbol{\rho}}_3 &= b\sqrt{m}\left(-1 - \frac{1}{2}(\cos\alpha + \cos\beta),\, \frac{1}{2}(\sin\alpha - \sin\beta)\right)^T
\end{aligned} \tag{2.10}$$

Hamiltonian in shape and rotation coordinates. To derive the Langevin equation in shape coordinates, we need a coordinate expression of the Hamiltonian. To this end, we note that[1]

$$\dot{\boldsymbol{\rho}}_i = \dot{Q}\tilde{\boldsymbol{\rho}}_i + Q\nabla\tilde{\boldsymbol{\rho}}_i\dot{s}\,,$$

or, in the body frame,

$$Q^T\dot{\boldsymbol{\rho}}_i = \boldsymbol{\omega} \times \tilde{\boldsymbol{\rho}}_i + \nabla\tilde{\boldsymbol{\rho}}_i\dot{s}\,.$$

In the last line, we have introduced $[\boldsymbol{\omega}\times] = Q^T\dot{Q} = -\dot{Q}^TQ$, $\boldsymbol{\omega} = (\omega, \omega)^T$ as the skew-symmetric 2×2 matrix defined by

$$[\boldsymbol{w}\times] = \begin{pmatrix} 0 & -w_1 \\ w_2 & 0 \end{pmatrix}\,,$$

[1]More precisely, given that $2\vartheta\tilde{\gamma} = \tilde{\sigma}\tilde{\sigma}$ we have $\mathbf{E}[\boldsymbol{P}] = 0$ where $\mathbf{E}[\cdot]$ is the expectation over all realizations of the driving white noise process. As a consequence, $\mathbf{E}[\boldsymbol{R}]$ is a conserved quantity.
[1]In the usual abuse of notation, we denote velocity vectors by an overdot, i.e., $v_{\boldsymbol{\rho}} = \dot{\boldsymbol{\rho}}$

where the skew-symmetry is implied by the fact that $Q^TQ = I$. Note that, by definition, $[\boldsymbol{w}\times]\boldsymbol{v} = \boldsymbol{w}\times\boldsymbol{v}$ is the cross product between two vectors $\boldsymbol{w},\boldsymbol{v}\in\mathbf{R}^2$. To proceed it is convenient to express the total energy in terms of positions and velocities, rather than positions and momenta. We find[2]

$$\begin{aligned}
E &= \frac{1}{2}\sum_{i=1}^{3}|\dot{\boldsymbol{\rho}}_i|^2 + \tilde{V}(\boldsymbol{\rho}) \\
&= \frac{1}{2}\sum_{i=1}^{3}\left\{\frac{\partial\tilde{\boldsymbol{\rho}}_i}{\partial s_k}\frac{\partial\tilde{\boldsymbol{\rho}}_i}{\partial s_l}\dot{s}_k\dot{s}_l + 2(\boldsymbol{\omega}\times\tilde{\boldsymbol{\rho}}_i)^T(\nabla\tilde{\boldsymbol{\rho}}_i\dot{s}) + |\boldsymbol{\omega}\times\tilde{\boldsymbol{\rho}}_i|^2\right\} + \tilde{V}(s) \\
&= \frac{1}{2}\sum_{i=1}^{3}\left\{\frac{\partial\tilde{\boldsymbol{\rho}}_i}{\partial s_k}\frac{\partial\tilde{\boldsymbol{\rho}}_i}{\partial s_l}\dot{s}_k\dot{s}_l + 2(\boldsymbol{\omega}\times\tilde{\boldsymbol{\rho}}_i)^T(\nabla\tilde{\boldsymbol{\rho}}_i\dot{s}) + |\boldsymbol{\omega}\times\tilde{\boldsymbol{\rho}}_i|^2\right\} + \tilde{V}(s) \\
&= \frac{1}{2}\sum_{i=1}^{3}\left\{\frac{\partial\tilde{\boldsymbol{\rho}}_i}{\partial s_k}\frac{\partial\tilde{\boldsymbol{\rho}}_i}{\partial s_l}\dot{s}_k\dot{s}_l + 2\boldsymbol{\omega}^T\sum_{j=1}^{2}\tilde{\boldsymbol{\rho}}_i\times\left(\frac{\partial\tilde{\boldsymbol{\rho}}_i}{\partial s_j}\right)\dot{s}_j + |\boldsymbol{\omega}\times\tilde{\boldsymbol{\rho}}_i|^2\right\} + \tilde{V}(s) \\
&= \frac{1}{2}\dot{s}^TG(s)\dot{s} + \omega B\dot{s} + \frac{1}{2}\Theta\omega^2 + \tilde{V}(s)
\end{aligned}$$

where we have used the convention $\tilde{V}(\boldsymbol{\rho}) = \tilde{V}(s,\theta) = \tilde{V}(s)$ and introduced the shorthands $G = (G_{ij})_{ij=1,2}$, $B = (B_1, B_2)$ and $\Theta > 0$ with

$$G_{ij} = \sum_{k=1}^{3}\left(\frac{\partial\tilde{\boldsymbol{\rho}}_k}{\partial s_i}\right)^T\frac{\partial\tilde{\boldsymbol{\rho}}_k}{\partial s_j}\,,\quad B_i = \sum_{l=1}^{2}\sum_{k=1}^{3}\tilde{\boldsymbol{\rho}}_{k,l}\times\left(\frac{\partial\tilde{\boldsymbol{\rho}}_{k,l}}{\partial s_i}\right)\,,\quad \Theta = \sum_{k=1}^{3}|\tilde{\boldsymbol{\rho}}_k|^2$$

Note that the total energy depends on θ only via the angular velocity $\omega = \dot{\theta}$. For reasons that will become clear in a second it is now convenient to introduce the *gauge potential* $A = (A_1, A_2)$ by $A = \Theta^{-1}B$ and define the 3×3 metric tensor

$$g = \begin{pmatrix} G & A^T\Theta \\ \Theta A & \Theta \end{pmatrix} = \begin{pmatrix} \mathbf{1} & \mathbf{0} \\ A & \mathbf{1} \end{pmatrix}^T\begin{pmatrix} C & \mathbf{0} \\ \mathbf{0} & \Theta \end{pmatrix}\begin{pmatrix} \mathbf{1} & \mathbf{0} \\ A & \mathbf{1} \end{pmatrix}. \tag{2.11}$$

Here $C = G - A^T\Theta A$ is the intrinsic shape space metric; it is intrinsic in that it does not depend on how the body frame is attached to the molecule, a property sometimes referred to as *gauge independence* [13]. The total energy now is

$$E = \frac{1}{2}\dot{s}^TC(s)\dot{s} + \frac{1}{2\Theta}L^2 + \tilde{V}(s)\,, \tag{2.12}$$

with $L = \omega + A\dot{s}$ being the angular momentum with respect to the body frame, in accordance with (2.2). Notice that under the condition of zero angular momentum, $L = 0$, the total energy still depends on the moment of inertia Θ via the shape space metric C.

The Hamiltonian can now be easily computed. Defining the conjugate momenta

[2]Note that $|\dot{\boldsymbol{\rho}}_i|^2 = |Q^T\dot{\boldsymbol{\rho}}_i|^2$, i.e., the kinetic energy is the same in the body frame or in the lab frame.

(u, η) to shape coordinates s and the angle θ in the canonical way,

$$u = \frac{\partial E}{\partial \dot{s}}\,, \quad \eta = \frac{\partial E}{\partial \omega}\,,$$

and using the factorization (2.11),

$$g^{-1} = \begin{pmatrix} \mathbf{1} & \mathbf{0} \\ -A & \mathbf{1} \end{pmatrix} \begin{pmatrix} C^{-1} & \mathbf{0} \\ \mathbf{0} & \Theta^{-1} \end{pmatrix} \begin{pmatrix} \mathbf{1} & \mathbf{0} \\ -A & \mathbf{1} \end{pmatrix}^T\,,$$

we find

$$\tilde{H} = \frac{1}{2}(u - A^T L)^T C^{-1}(u - A^T L) + \frac{1}{2\Theta} L^2 + \tilde{V}(s)\,, \tag{2.13}$$

where we have taken advantage of the fact that the angular momentum L is indeed the conjugate momentum to θ, i.e., it holds that $L = \eta$.

Remark. When the configuration space is 3-dimensional, i.e. when $d = 3$, a popular choice for describing the overall orientation of the molecule is in terms of Euler angles. There are two problems with this choice: firstly, the angular momenta are not conjugate to the Euler angles, secondly, Euler angles lead to singularities in the parameterization of the rotation group (as any other 3-dimensional global parameterization). As fas as we know, the problem of non-conjugacy cannot be avoided, which, however, is mainly a problem for the physical interpretation of the falling cat effect, rather than for its mathematical analysis. The second problem can be overcome by using singularity-free coordinate charts, e.g. unit quaternions or rotation matrices. But because these parameterizations are based on embeddings of the 3-dimensional rotation group into a higher-dimensional space (e.g. 4-dimensional in case of the unit quaternions), they involve additional constraints that would make the mathematical analysis of the Langevin equation more involved.

3. Langevin equation in shape space

We want to derive the Langevin equation in shape and angular coordinates. Calling $\boldsymbol{x} = (s, \theta)$ and $\boldsymbol{y} = (u, L)$, the Langevin equation is (2.7) with $\tilde{H}$ given by (2.13) and coordinate dependent friction and noise coefficients given by

$$\tilde{\gamma} = \frac{\gamma}{m} \begin{pmatrix} G & A^T\Theta \\ \Theta A & \Theta \end{pmatrix}\,, \quad \tilde{\sigma} = \frac{\sigma}{\sqrt{m}} \begin{pmatrix} C^{1/2} & A^T\Theta^{1/2} \\ 0 & \Theta^{1/2} \end{pmatrix}$$

Even though the angular momentum is no longer a conserved quantity as in the deterministic case discussed in Section 2, it is zero on average when the system is in equilibrium. This property follows from (2.6) which implies that the stationary distribution of the Langevin equation (2.7) has the density

$$\tilde{\rho}(\boldsymbol{x}, \boldsymbol{y}) = \frac{1}{\tilde{Z}} \exp(-\vartheta^{-1}\tilde{H}(\boldsymbol{x}, \boldsymbol{y}))\,,$$

which shows that L is Gaussian with zero mean. Here $\tilde{Z}$ is again a normalization constant for the translation-reduced probability density.

Geometric phase. To study the effect of the internal motion of the molecule on its orientation, we write down the equation for the conjugate pair (θ, L),

$$\begin{aligned} \dot{\theta} &= (AC^{-1}A^T - \Theta^{-1})L - AC^{-1}u \\ \dot{L} &= -\frac{\gamma}{m}L + \sigma\sqrt{\frac{\Theta}{m}}\xi\,, \end{aligned} \tag{3.1}$$

where ξ is one-dimensional Gaussian white noise. From the second equation of (3.1) we recognize L as the Ornstein-Uhlenbeck process. Keeping the other variables fixed—we remind the reader that the equation for L is still coupled to the shape equations, for $\Theta = \Theta(s)$—it follows that L is a Gaussian process with mean

$$\mathbf{E}[L(t)] = e^{-\frac{\gamma t}{m}}L(0)$$

and variance

$$\mathbf{E}[(L(t) - \mathbf{E}[L(t)])^2] = \frac{\sigma^2\Theta}{2\gamma}\left(1 - e^{-\frac{2\gamma t}{m}}\right).$$

We see that $\mathbf{E}[L(t)]$ quickly converges to 0 whenever γ/m is not too small. If moreover the temperature $\vartheta = \sigma^2/(2\gamma)$ in the system is small, then L will have small variance too, which justifies to set $L = 0$ in the first equation of (3.1), by which we obtain the following result

$$\dot{\theta} \approx -AC^{-1}u\,. \tag{3.2}$$

But under the condition of zero angular momentum, we have that $\dot{s} = C^{-1}u$, hence (3.2) is stochastic reformulation of (2.3) for the Langevin equation. Our findings will be confirmed by numerical studies in Section 4 below.

Finally, replacing L and L^2 in the Langevin equation by its stationary mean and covariance, we obtain the Langevin equation on shape space

$$\begin{aligned} \dot{s} &= \frac{\partial K}{\partial u} \\ \dot{u} &= -\frac{\partial K}{\partial s} - \frac{\gamma}{m}C\frac{\partial K}{\partial u} + \frac{\sigma}{\sqrt{m}}C^{1/2}\boldsymbol{\zeta}\,, \end{aligned} \tag{3.3}$$

where $\boldsymbol{\zeta}$ is two-dimensional uncorrelated Gaussian white noise and

$$K(s,u) = -\vartheta\log\int_{S_1\times\mathbf{R}}\tilde{\rho}(s,\theta,u,L)\,d\theta dL$$

is the shape space free energy. The free energy is not, as one could guess from the deterministic case, the Hamiltonian for $L = 0$. It rather contains an additional temperature-dependent correction term that mimics coriolis-type forces arising from the random fluctuations of the angular momentum L (see the discussion in Sec. 3.1 below).

Using the fact that the equilibrium momentum distribution is Gaussian and completing the square in the expression for the kinetic energy, we find

$$K = \frac{1}{2}u^TG^{-1}u + U_\vartheta(s)\,. \tag{3.4}$$

with the pseudo-metric tensor G that is induced by the embedding of shape space into the Cartesian coordinate space of the semi-flexible molecule, i.e. the restriction of the Euclidean metric to the submanifold $\mathbf{T}^2 \subset \mathbf{R}^4$, and the effective potential

$$U_\vartheta = \tilde{V} + \frac{\vartheta}{2} \log(\Theta^{-1} + AC^{-1}A^T)\,. \tag{3.5}$$

(We have omitted additive constants in the potential.) The metric coefficient and thus the free energy can be computed explicitly, but as the actual coordinate expressions of the metric tensor are not very informative, involving trigonometric functions, they have been moved to the appendix.

Remark. An equivalent representation of the correction potential $F := U_\vartheta - \tilde{V}$ is obtained by using the Woodbury identity [6, Sec. 2.1.3] for the inverse of the Schur-complement-like matrix $\Theta^{-1} + AC^{-1}A^T$:

$$F = -\frac{\vartheta}{2} \log(\Theta - \Theta A G^{-1} A^T \Theta)\,.$$

3.1. *Discussion of the temperature-dependent correction potential*

It is interesting to note that even though the Langevin dynamics under equilibrium conditions (2.8) satisfies $L = 0$ on average, or, more precisely $\mathbf{E}[L] = 0$, the free energy K is very different from the zero-angular momentum Hamiltonian, viz.,

$$\tilde{H}|_{L=0} = \frac{1}{2} u^T C^{-1} u + V(s)\,,$$

where $C = G - A^T \Theta A$. The reason for this is that a random variable L is almost surely constant if and only if it has zero variance, i.e. if and only if $\mathbf{E}[L^2] = 0$. But this is not the case here, for L is approximately Gaussian with variance proportional to ϑ, which may not be small.

As has been discussed in [13], the pseudo-metric tensor G that appears in the kinetic energy of the effective Hamiltonian K does depend on the frame and thus has no intrinsic meaning as a shape space metric tensor, whereas C is independent of the chosen frame or reference configuration of the molecule. Here it is the temperature dependent, so-called *Fixmann potential* that guarantees that the resulting shape space equilibrium distribution is gauge invariant, even though the effective Hamiltonian is not. Indeed, by definition of the free energy, it follows that

$$\exp(-\vartheta^{-1} K) = \int_{S_1 \times \mathbf{R}} \exp(-\vartheta^{-1} \tilde{H})\, d\theta dL$$

which entails

$$\exp(-\vartheta^{-1} U) \sqrt{\det G} \propto \exp(-\vartheta^{-1} V) \sqrt{\det g}\,.$$

The latter is equivalent to

$$\frac{\det G}{\det g} \propto \Theta - \Theta A G^{-1} A^T \Theta$$

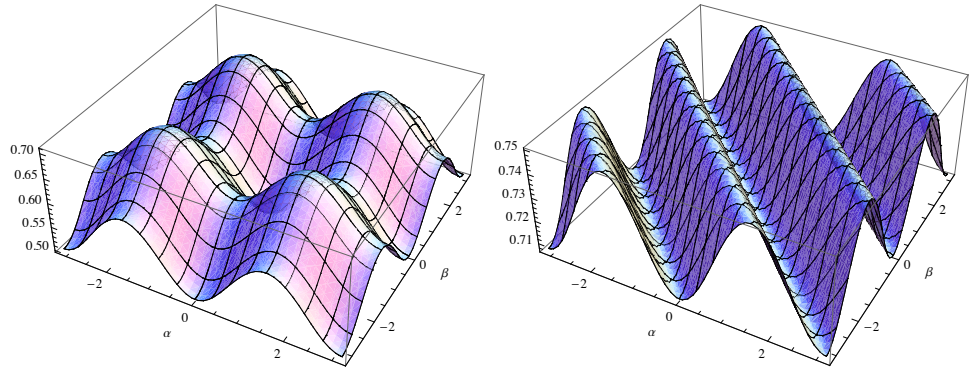

Figure 4. Square rooted matrix volumes of ambient space metric tensor g (left panel) and induced shape space metric tensor G (right panel). The scaling of the z-axis is arbitrary.

and highlights the interpretation of the Fixman potential as an entropic correction that accounts for the difference between the matrix volumes of the induced shape space metric G and its ambient space metric (2.11). We refer to the seminal article [5] by Fixman (to whom the potential owes his name) or the related works [3, 9] for a discussion of the Fixman potential related to the realization of holonomic constraints. It should be stressed that the free energy as well as the Fixman potential are generally gauge-dependent, as has been discussed in, e.g., [8].

The square roots of the matrix volumes elements of both restricted (i.e., constrained) metric and full tensor are shown in Figure 4. The entropic meaning of the matrix volume is such that, if the molecular potential $\tilde{V}$ is ignored, regions of large matrix volume correspond to regions of high probability in the configurational ensemble, just because these configurations make up a larger part of the possible configurations of a molecule that is free to rotate otherwise; in our case the entropically least favourable (i.e. least likely) configuration is the configuration $\alpha = \beta = 0$, when the molecule is completely straight. Note that the actual form of the induced metric tensor G is arbitrary, as it changes with the choice of the body frame.[1] For comparison, Figure 5 shows the Fixman potential that has four well pronounced minima where the full system (including rotations) has large entropic wells that correspond to a large matrix volume.

Remark. The fact that that the free energy K is different from the symmetry-reduced Hamiltonian $\tilde{H}|_{L=0}$ also underlines that it matters whether we first remove the heat bath in the Langevin equation (2.5) equation by setting $\gamma, \sigma = 0$ and then factor out the orientation and translation variables, in accordance with what is done for deterministic systems, or remove the heat bath afterwards. In the latter case the factor multiplying the Fixman potential can be replaced by the average kinetic energy per degree of freedom in the microcanonical ensemble, in accordance with the equipartition theorem. The two operations do not commute, because the underlying thermodynamic ensembles, microcanonical or canonical, are manifestly different.

[1] Geometrically, the choice of frame corresponds to a 2-dimensional section in the 4-dimensional configuration manifold of our semi-flexible molecule. One such choice, that even makes the section locally flat, follows from the Eckart conventions [4], for which the induced metric is the Euclidean metric.

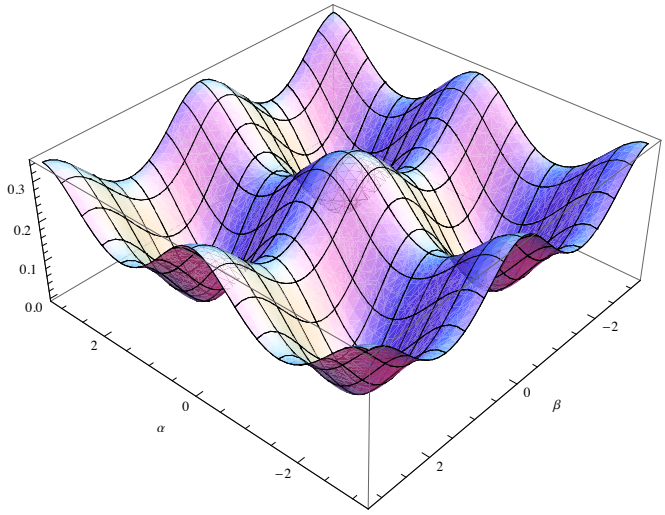

Figure 5. Fixman potential $F := U_\vartheta - \tilde{V}$ as a function of the two shape variables. The four wells of the Fixman potential correspond to the most probable configurations around $(\alpha, \beta) = (\pm\pi/2, \pm\pi/2)$ that the molecule adopts. (The scaling of the z-axis is arbitrary.)

4. Numerical tests

4.1. *Falling cat effect in vacuum and in solvent*

In this section, we carry out numerical simulations to test the formulations presented in the previous sections by taking the example of the prototypical model of the four-atom molecule. We focus here on the coupling between the shape changes and rotations of the planar four-atom chain under Langevin dynamics.

Numerical implementation. In our numerical study, the lengths of all the three bonds are fixed to b. The two bending angles α and β are controlled by a scleronomic constraint function for the bending angles. Thus, we solve the following underdamped Langevin equations with constraints:

$$\begin{aligned} \dot{\boldsymbol{q}} &= \boldsymbol{v}, \\ m\dot{\boldsymbol{v}} &= -\gamma\boldsymbol{v} - \nabla \boldsymbol{f}_{\text{bond}}(\boldsymbol{q})\boldsymbol{\lambda}_{\text{bond}} - \nabla \boldsymbol{f}_{\text{angle}}(\boldsymbol{q}, t)\boldsymbol{\lambda}_{\text{angle}} + \sigma\boldsymbol{\xi}(t) \\ 0 &= \boldsymbol{f}_{\text{bond}}(\boldsymbol{q}) \\ 0 &= \boldsymbol{f}_{\text{angle}}(\boldsymbol{q}, t)\,, \end{aligned} \tag{4.1}$$

where $\boldsymbol{f}_{\text{bond}}$, $\boldsymbol{f}_{\text{angle}}$ are defined by

$$\begin{aligned} \boldsymbol{f}_{\text{bond}}(\boldsymbol{q}) &= \begin{pmatrix} |\boldsymbol{q}_1 - \boldsymbol{q}_2|^2 - b^2 \\ |\boldsymbol{q}_2 - \boldsymbol{q}_3|^2 - b^2 \\ |\boldsymbol{q}_3 - \boldsymbol{q}_4|^2 - b^2 \end{pmatrix} \\ \boldsymbol{f}_{\text{angle}}(\boldsymbol{q}, t) &= \begin{pmatrix} (\boldsymbol{q}_3 - \boldsymbol{q}_2)\cdot(\boldsymbol{q}_2 - \boldsymbol{q}_1) \\ (\boldsymbol{q}_4 - \boldsymbol{q}_3)\cdot(\boldsymbol{q}_3 - \boldsymbol{q}_2) \end{pmatrix} - \begin{pmatrix} b^2\cos\alpha(t) \\ b^2\cos\beta(t) \end{pmatrix}, \end{aligned} \tag{4.2}$$

Here $\boldsymbol{q}$ and $\boldsymbol{v}$ are 8-dimensional position and velocity vectors, m is the atomic mass, $\boldsymbol{\xi}$ is the vector of random forces (Gaussian white noise), γ is the friction coefficient, $\sigma = \sqrt{2\vartheta/\gamma}$ the friction coefficient, $\boldsymbol{\lambda}_{\text{bond}}$ is the three-dimensional vector of Lagrange multipliers for the constraint on the bond length, and $\boldsymbol{\lambda}_{\text{angle}}$ is a

two-dimensional vector of Lagrange multipliers for the constraints for the bending angles; $\boldsymbol{f}_{\text{bond}}$ and $\boldsymbol{f}_{\text{angle}}$ are the constraint functions for the bonds and for the angles; the bending angles are controlled via the time-dependent constraint function $\boldsymbol{f}_{\text{angle}}(\boldsymbol{q}, t)$. For the numerical integration of (4.1) we use the stochastic RATTLE algorithm as described in [19]; cf. also [12]

Motions in vacuum vs. motions in solvent. We have first tested the numerical shape control scheme without noise nor friction, i.e. for $\gamma = 0$ and $\sigma = 0$. Figure 2 shows the results for the time evolution of the configuration of the four-atom chain for the cyclic shape change prescribed in Fig. 3. Since noise and friction are absent, this is regarded as the cyclic shape change in vacuum. The solid curve (red) in the left panel of Figure 6 shows the time evolution of the orientation θ of the body frame in the course of this cyclic shape change. We see that, after the cyclic shape change, the orientation of the body frame differs from the initial one and coincides with the theoretically predicted value $\theta = 11.786^\circ$ as noted before. The solid curve (red) in the right panel of Figure 6 shows the total angular momentum of the system during the cyclic shape change. One can readily check that the the total angular momentum $L = 0$ is strictly preserved throughout the process. All these results confirm that our numerical implementation of the RATTLE algorithm with time-dependent constraints works well and correctly reproduces the "falling cat" effect.

Next we study the geometric phase effect and shape dynamics under Langevin dynamics based on (4.1)–(4.2). The dotted curves in Figure 6(a) show the time evolutions of the orientation of the body frame θ during the cyclic shape change (see Figure 3) for 50 independent realization of the Langevin dynamics. For all realizations the parameters were set as $\gamma = 0.1$, $m = 1$, and temperature $\vartheta = 1$. Because of the presence of noise, the time evolutions of θ are different for different trajectories. However, we can clearly see the tendency that on average the stochastic trajectories follow the deterministic trajectory under the conditions of zero total angular momentum. Moreover the mean value of the final orientation of the body frame, averaged over the 50 realizations, is almost the same as the theoretical value $\theta = 11.786^\circ$. Hence we conclude that the geometric phase effect survives even under the noisy Langevin dynamics as equation (3.1) theoretically predicts. The dotted curves in Fig. 6(b) are the time evolution of the total angular momentum of the system for the same 50 realizations as in Figure 6(a). As expected the total angular momentum is fluctuating around $L = 0$.

Dependence on Langevin parameters. We now study the dependence of the "falling cat" effect on atomic masses m, friction γ, temperature ϑ, and the speed of shape change. The solid curves (red) in Figure 7 show the distribution of the final orientation of the body frame after the cyclic shape change for the parameter values $\gamma = 0.1$, $m = 1$, and $\vartheta = 1$. Note that solid red curves in Figure 7 are the same. The total time for completing the cyclic shape change is 1000 (in absolute units) where each of the four steps of the shape change in Figure 3 (from (a) to (e)) takes 250 time units. We see from the solid curves in Figure 7 that the final distribution of the orientation of the body frame is roughly a Gaussian, whose peak in located at around $\theta = 11.786^\circ$, which is the predicted geometric phase under zero angular momentum. We regard this result for the parameter values of $\gamma = 0.1$, $m = 1$, and $\vartheta = 1$ as a "benchmark".

We have then investigated how the distribution of the final orientation of the body frame after the cyclic shape changes for various Langevin parameters. Figure

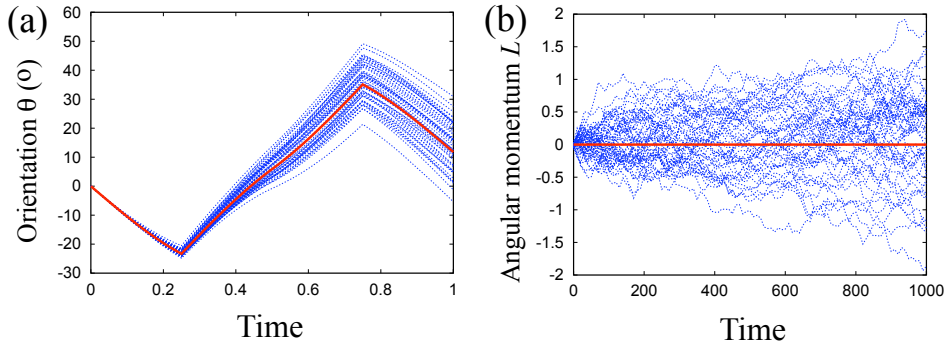

Figure 6. On-average preservation of the total angular momentum. The thick solid line (red) in (a) shows time vacuum evolution of the orientation of the body frame under a cyclic shape change described in Figure 3. The thick solid line (red) in (b) is the corresponding time evolution of the total angular momentum of the system, which is zero throughout the process. The blue dotted lines in (a) show 50 typical realization of the orientation of the body frame under cyclic shape change and Langevin dynamics. The blue dotted lines in (b) show the corresponding total angular momenta.

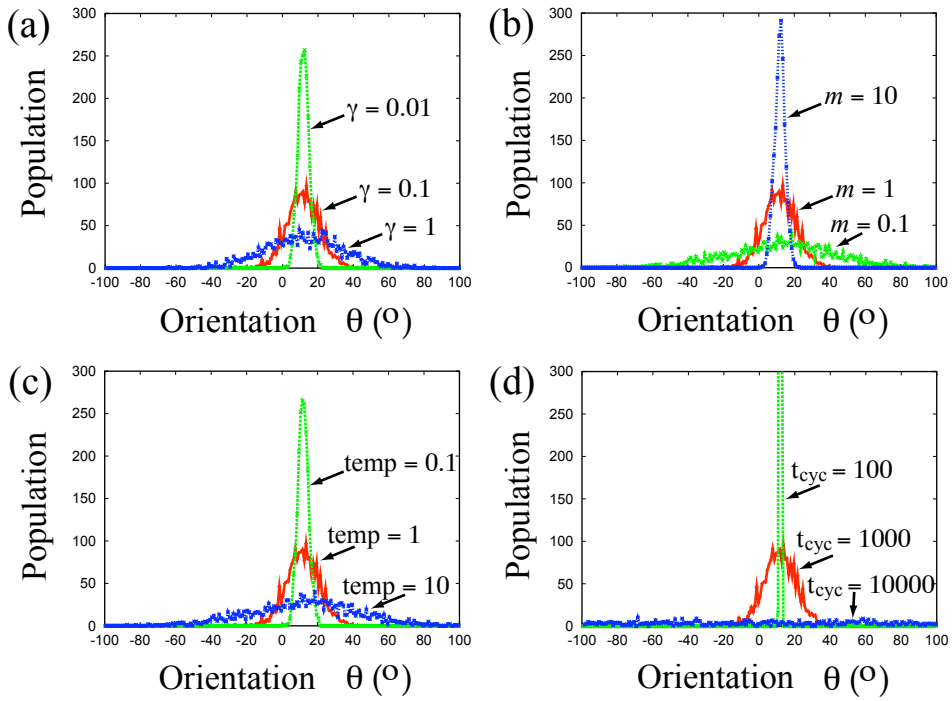

Figure 7. Distributions for the final orientation of the body frame θ after the cyclic shape change under Langevin dynamics for different parameters: (a) is for different friction coefficient, (b) is for different atomic masses, (c) is for different temperature, (d) is for varying shape change rates.

7(a) compares the final distribution of the body frame for the three different values of friction coefficient, $\gamma = 0.01$ (green), $\gamma = 0.1$ (red), and $\gamma = 1$ (blue). All other parameters are set to the "benchmark" values defined above, i.e. $m = 1$, and $\vartheta = 1$. We see from Figure 7(a) that the width of the distribution of the final orientation of the body frame becomes wider as the friction coefficient increases. Thus strong friction seems to obscure the geometric phase effect.

Figure 7(b) compares the distributions of the final orientation of the body frame for the three different values of atomic masses, $m = 0.1$ (green), $m = 1$ (red), $m = 10$ (blue). As opposed to the friction coefficient, large masses of atoms make the geometric phase effect stand out. That is, the atomic masses have the behave inversely to the friction coefficients which is plausible as they appear as γ/m in the

shape-rotation transformed Langevin equation.

Figure 7(c) displays the distributions of the final orientation for the three different temperatures, $\vartheta = 0.1$ (green), $\vartheta = 1$ (red), and $\vartheta = 10$ (blue). We observe that the effect of temperature resembles the effect of the friction coefficient, which is in accordance with the fuctuation-dissipation theorem: high temperature corresponds to high noise in the Langevin dynamics, so that the orientation dynamics becomes essentially a the random walks on S^1; the orientation samples its invariant measure (which is the Haar measure on SO(3) for a three-dimensional molecule).

Finally Figure 7(d) shows the distributions of the orientations for different rates at which the cyclic shape change is done. The distributions in green, red, and blue are the results for the cyclic shape changes that took $t_{\rm cyc} = 100$, $t_{\rm cyc} = 1,000$, and $t_{\rm cyc} = 10,000$ units of time. The distribution in green is the result for the fastest shape change and that in blue corresponds to the slowest shape change. We clearly see that fast shape change of the system preserves the geometric phase effect well, whereas it totally vanishes if the shape change of the system is slow. This behaviour can be explained by noting that the orientation is basically adiabatic with respect to to the parameter change in shape space. It is noteworthy that also the net amount of orientational shift depends on the velocity of shape change in the Langevin dynamics. This is different from the dynamics in vacuum, where the net orientational shift does not depend on the velocity of shape change.

4.2. *Probability distribution in shape space*

We have further sampled the probability distribution in shape space. We numerically simulate the Langevin dynamics of the four-atom molecule in Figure 1 using the RATTLE algorithm, but, this time, we impose only the constraints for the bond lengths, $\boldsymbol{f}_{\rm bond}(\boldsymbol{q})$ and remove the bending angle constraints $\boldsymbol{f}_{\rm angle}(\boldsymbol{q}, t)$. Figure 8

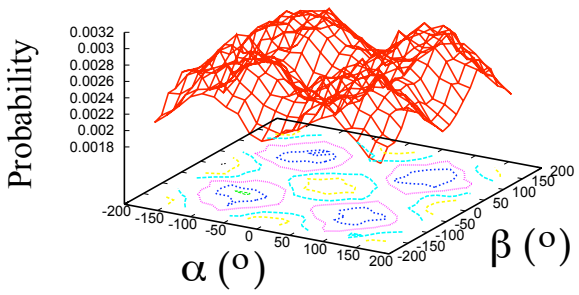

Figure 8. Probability distribution in shape space in the Langevin dynamics of the four-atom molecule in Fig. 1. This result should be compared with Figure 4.

shows the result for the empirical shape space probability distribution which nicely agrees with the theoretical prediction (see Figure 4). The empirical distribution exhibits four pronounced peaks around $(\alpha, \beta) = (\pm\pi/2, \pm\pi/2)$, a finding which is is consistent with the four minima of the Fixman potential shown in Figure5. The probability distribution in Figure 8 is also consistent with Fig. 5 in that the straight configuration of the molecule, where $\alpha = \beta = 0$ has the lowest entropy.

5. Conclusions and future directions

We have studied geometric phase effects in small molecular cluster in a stochastic heat bath. As a simple model system that displays interesting geometric behaviour during conformational transitions we have analysed the Langevin dynamics of a

semiflexible, planar four-atomic molecule, which internal configurations are completely specified by its two bond angles. Following the symmetry-reduction procedure that is usually employed for deterministic Hamiltonian systems (i.e. *in vacuo*), we have derived a symmetry-reduced Langevin equation by eliminating overall translation and rotation component. The main difference here is that the angular momentum of the molecule is not a conserved quantity, and hence the system cannot be reduced by setting the angular momentum constant (typically zero). If, however, the system is in equilibrium (i.e., when friction and noise coefficients in the Langevin equation satisfy the fluctuation-dissipation relation), the angular momentum is Gaussian with stationary mean and variance, in case of which the angular momentum is conserved on average. The symmetry-reduced Langevin equation is then obtained by averaging over the stationary fluctuations. We found that the resulting free energy is different from its reduced deterministic counterpart; one of the features of the free energy is a temperature dependent correction potential (Fixman potential) that arises from the averaging procedure and mimics the influence of the eliminated angular motion; moreover the free energy is, other than the reduced Hamiltonian in the deterministic setting, gauge dependent and changes with the definition of the body frame that is attached to the molecule. We have numerically verified that at low friction, the stochastic system behaves basically as the deterministic "falling cat". The geometric phase is sharply peaked around its predicted value. But in contrast to the vacuum situation, the falling cat effect depends on the rate at which the shape is changes. Specifically, we found that the phase distribution becomes broader as the rate goes down which may have significant implication for the control of such systems (depending on whether controls are fast or slow). We have further observed that the falling cat effect is obscured at high friction, but it is unclear whether the phase distribution becomes just too broad to get statistically significant data or whether is the effect disappears in the overdamped limit.

Future research should be devoted to a careful analysis of the overdamped equation and its reduction; an interesting question could be whether, e.g., the order of the limiting procedure and the symmetry reduction matters, or if the orientational degree of freedom play a role during conformational transitions and can reduce metastability. Another interesting question in this respect is the control of conformational transitions by external forcing, especially the question whether an optimal control strategy for the molecule's shape has to take into account overall rotations. Last but not least, it remains to generalize our considerations to the 3-dimensional case and more general multibody systems.

References

[1] E. Belbruno. *Capture Dynamics and Chaotic Motions in Celestial Mechanics*. Princeton University Press, 2004.

[2] M. V. Berry. Quantal phase factors accompanying adiabatic changes. *Proc. R. Soc. A.*, 392:45–57, 1984.

[3] G. Ciccotti and J.P. Ryckaert. Molecular dynamics simulation of rigid molecules. *Comput. Phys. Rep.*, 4:345–392, 1986.

[4] Carl Eckart. Some studies concerning rotating axes and polyatomic molecules. *Phys. Rev.*, 47:552–558, 1935.

[5] M. Fixman. Classical statistical mechanics of constraints: a theorem and applications to polymers. *Proc. Natl. Acad. Sci. USA*, 71:3050–3053, 1974.

[6] G.H. Golub and C.F. Van Loan. *Matrix Computations*. Johns Hopkins University Press, Baltimore, 1996.

[7] C. Hartmann. *Model Reduction in Classical Molecular Dynamics*. PhD Thesis, Fachbereich Mathematik und Informatik, Freie Universität Berlin, 2007.

[8] C. Hartmann, J.C. Latorre, and G. Ciccotti. On two possible definitions of the free energy for collective variables. *Eur. Phys. J. Special Topics*, 200:73–89, 2011.
[9] E. Helfand. Flexible vs rigid constraints in statistical mechanics. *J. Chem. Phys.*, 71:5000–5007, 1979.
[10] T. R. Kane and M. P. Scher. A dynamical explanation of the falling cat phenomenon. *Int. J. of Solids Structures*, 5:663–666, 1969.
[11] Scott D. Kelly and Richard M. Murray. Geometric phases and robotic locomotion. *J. Robotic Syst.*, 12:417–431, 1995.
[12] B. Leimkuhler and S. Reich. *Simulating Hamiltonian Dynamics*. Cambridge University Press, Cambridge, 2004.
[13] Robert G. Littlejohn and Matthias Reinsch. Gauge fields in the separation of rotations and internal motions in the n-body problem. *Rev. Mod. Phys.*, 69:213–276, 1997.
[14] J.E. Marsden, G. Misiolek, J.-P. Ortega, M. Perlmutter, and T.S. Ratiu. *Hamiltonian Reduction by Stages*. Lecture Notes in Mathematics, Vol. 1913. Springer, 2007.
[15] R. Montgomery. Gauge Theory of the Falling Cat. In Michael J. Enos, editor, *Dynamics and Control of Mechanical Systems: The Falling Cat and Related Problems*, volume 1 of *Fields Institute Communications*, pages 193–218. American Mathematical Society, 1993.
[16] S. Pancharatnam. Generalised theory of interference and its applications. *P. Indian Acad. Sci. A*, 46:1–18, 1957.
[17] E. M. Purcell. Life at low reynolds number. *Am. J. Physics*, 45:3–11, 1977.
[18] Aaron Sayvetz. The kinetic energy of polyatomic molecules. *J. Chem. Phys.*, 7:383–389, 1939.
[19] E. Vanden-Eijnden and G. Ciccotti. Second-order integrators for Langevin equations with holonomic constraints. *Chem. Phys. Lett.*, 429:310–316, 2006.
[20] Bryan M. Wong, Ryan L. Thom, and Robert W. Field. Accurate inertias for large-amplitude motions: improvements on prevailing approximations. *J. Phys. Chem. A*, 110:7406–7413, 2006.
[21] Tomohiro Yanao, Wang S. Koon, and Jerrold E. Marsden. Mass effects and internal space geometry in triatomic reaction dynamics. *Phys. Rev. A*, 73:052704, 2006.
[22] Tomohiro Yanao, Wang Sang Koon, and Jerrold E. Marsden. Intramolecular energy transfer and the driving mechanisms for large-amplitude collective motions of clusters. *J Chem. Phys.*, 130:144111, 2009.
[23] John Z. H. Zhang. *Theory and application of quantum molecular dynamics*. World Scientific, 1999.

Appendix A. More coordinate expressions

Both the intrinsic shape space metric and the shape space free energy can be computed directly. The metric tensor G that is induced on the shape space $\mathbf{T}^2$ by restricting the Euclidean metric has the components

$$G_{11} = G_{22} = \frac{3mb^2}{4}\,, \quad G_{12} = G_{21} = \frac{mb^2}{4}\cos(\alpha+\beta)\,.$$

Together with the explicit expressions for the gauge potential,

$$A_1 = \frac{3 + 2\cos\alpha + \cos(\alpha+\beta)}{10 + 4\cos\alpha + 4\cos\beta + 2\cos(\alpha+\beta)}$$
$$A_2 = \frac{3 + 2\cos\beta + \cos(\alpha+\beta)}{10 + 4\cos\alpha + 4\cos\beta + 2\cos(\alpha+\beta)}\,,$$

and the moment of inertia,

$$\Theta = mb^2\left(\frac{5}{2} + \cos\alpha + \cos\beta + \frac{1}{2}\cos(\alpha+\beta)\right)\,,$$

the coefficients of the intrinsic metric on shape space are readily found to be

$$C_{11} = \frac{3mb^2}{4} - \frac{mb^2(3+2\cos\alpha+\cos(\alpha+\beta))^2}{40+16\cos\alpha+16\cos\beta+8\cos(\alpha+\beta)}$$

$$C_{22} = \frac{3mb^2}{4} - \frac{mb^2(3+2\cos\beta+\cos(\alpha+\beta))^2}{40+16\cos\alpha+16\cos\beta+8\cos(\alpha+\beta)}$$

$$C_{12} = \frac{mb^2\cos(\alpha+\beta)}{4} - \frac{mb^2(3+2\cos\alpha+\cos(\alpha+\beta))(3+2\cos\beta+\cos(\alpha+\beta))}{40+16\cos\alpha+16\cos\beta+8\cos(\alpha+\beta)}$$

$$C_{21} = C_{12}\,.$$